

Performance-based Seismic Evaluation of Vertically Irregular Moment Resisting Reinforced Concrete Frames using Nonlinear Statics Analysis

Abdul Mabood^{1*}, Mohd.Zameerruddin², P.M. Shimpale³

¹PG Student, Department of Civil Engineering, MGM's College of Engineering Nanded, Maharashtra, India.,

²Associate Professor, Department of Civil Engineering, MGM's college of Engineering, Nanded Maharashtra, India.

³Associate Professor, Department of Civil Engineering, MGM's college of Engineering, Nanded, Maharashtra, India.

Received Date: 02 May 2021

Revised Date: 04 June 2021

Accepted Date: 15 June 2021

Abstract

Nonlinear static procedures are used mainly for evaluation of the capacity of structures subjected to the seismic loads. During the seismic events reinforced concrete structures get damaged or collapsed. These damages happen due to the improper distribution of structural mass, structural stiffness and structural strength. In the structural irregular frames damages appears along the section which are geometrically unstable. This vulnerability of the irregular frame has caused discomfort among the stakeholders, especially for the multi-storeyed structures. In this study, we had performed nonlinear static analysis of the irregular frames, typically representing the vertical irregularities. The engineering demand parameters such as base shear, displacement, ductility, stiffness and inter-storey displacement were used to evaluate the performance of these frames. In addition an attempt has been made to correlate the damage state of frames with the identified performance level described in the performance-based seismic design documents.

Keywords - Structural Irregularities, Nonlinear Static Procedures, Example MRFs, Engineering Demand Parameters

INTRODUCTION

The seismic events which happened all over the world had destructive effects on the structures, which has forced the professional structural designers to implement the earthquake resistant design of the structures for safety of life and usage of structures [Ghobarah A, 2001; Zameeruddin and Sangle, 2016]. The scarcity of the availability of residential land and increase in the cost of the construction, especially in the urban areas has led towards the development of the multi-storeyed structures. The behaviour of multi-storeyed structure under the seismic loads depends on structural configurations. Irregular structural configurations either in plan or elevation are the major causes of failures during seismic events [Siva et al., 2019].

The earthquake resistant design methodologies

described in the present seismic codes are not capable to address the inelastic behaviour of reinforced concrete sections subjected to inelastic incursion. These codes provide the indirect approach of applying modification factor to the strength and displacements to take care of inelastic incursion [Mondal et al., 2013]. The predictive method of design available in the Performance-based Seismic Design (PBSD) documents proved to be the best alternative towards this code based procedures [FEMA 445, 2005; Zameeruddin and Sangle, 2021].

Performance evaluation procedure defined in PBSD documents are based on the nonlinear static or nonlinear dynamic analysis procedures. Due to ease in its procedure, the nonlinear static methods have become more common among the practicing engineers. The performance evaluation procedures based on the nonlinear static method include; (a) Capacity Spectrum Method (CSM) and Displacement Coefficient Method (DCM). [ATC 40, 1996; FEMA 273, 1996; FEMA 356, 2000; ASCE/SEI 41, 2007; Zameeruddin and Sangle, 2021; Boroujeni ARK 2013].

In PBSD the performance of the structure is evaluated on the basis of the damages sustained by structural and non-structural component. These performance levels are identified as operational levels, immediate occupancy, life safety range and collapse prevention. The performance analysis results into the collapse mechanisms which show the yielding of structural components, but are not capable to provide any damage value.

In this study, an attempt has been made to assess the performance of example moment resisting frames (MRFs) with different irregular configurations subjected to the lateral load patterns as described in the IS 1893 [2002]. The performance assessment includes parametric studies on fundamental period, roof displacement, inter-story drift ratio, and base shear. In addition, we had attempted to find the global damage



value by using the results obtained from PBSB and integrate it with the performance levels.

STRUCTURAL IRREGULARITIES

Modernization in the housing and infrastructure sector has raised the demand of multi- storeyed structures. To meet the minimum standards of the floor space ratio of multi- storeyed structures, irregular structural configuration has become a common practice. This had resulted in the construction of buildings with irregular distributions of mass, stiffness and strength along the height of the building [Bhosale et al., 2017; Soni and Mistry, 2006].

In IS 1893:2002 various irregularities have been mentioned. There are two categories of irregularities: vertical and horizontal. Table 1 summarizes all such classifications. The present study considers vertical irregularities in multi-storeyed structures. In general three forms of the vertical irregularities are being in practice for the construction of multi-storeyed structures. These include (a) set-back buildings, (b) buildings with floating columns, (c) in plan discontinuity and (d) open ground storey. Figure 1 shows the vertical geometric irregularity as per IS 1893:2002.

When such multi-storeyed structures are located in a high seismic zone, the seismic performance evaluation becomes more challenging. The methods of quantitative performance evaluation given in present codes of practice for the irregular multi-storeyed structures listed in Table 1 are not always supported by the structural characteristics. Most seismic codes suggest the use of dynamic analysis for estimation of the lateral load distribution over the structure (may use the elastic time history or elastic response spectrum analysis). To understand the nonlinear response of the structure using a dynamic analysis is a complex job, hence it is not preferred in the common design practice. Comparatively non-linear static procedures (NLSP) are simplest one, hence found to be common in the design practice. The present study aims to have a parametric study of engineering demand parameters using results obtained NLSPs. Also a damage indicator is being proposed, to assess the damage state of structure at various performance levels stated in PBSB.

NONLINEAR STATIC PROCEDURES

Contribution of research and experimental studies done in the field of seismic engineering has improved the seismic design and assessment procedures. With the intention to communicate the safety-related decisions to the stakeholders, the design engineers have shifted their focus towards the predictive methods of the seismic design. This resulted into the development of PBSB [Zameeruddin and Sangle 2017a].

The developments in the PBSB can be traced through the publication of the documents; The first generation documents (ATC 40 and FEMA 273), Second generation document (FEMA 356), and Next-generation document (FEMA 440 and FEMA 445). The PBSB document recommends various analysis methods for estimation of the seismic response of reinforced concrete structures, as

presented in the Table 2 [Zameeruddin and Sangle, 2021; Boroujeni ARK 2013].

Table 2: Various analysis procedures to estimate seismic responses recommended by PBSB

Type of Analysis	Usual Name	Dynamic Effect	Material Nonlinearity
Linear Statics	Equivalent static	NO	NO
Linear Dynamic	Response spectrum	YES	NO
Nonlinear Statics	Pushover	NO	YES
Nonlinear Dynamic	Time history	YES	YES

These documents provided two approaches of performance-based seismic (PBSE) evaluation: (a) capacity spectrum method and (b) displacement coefficient method. PBSE procedures use NLSP procedure to evaluate the capacity of structure subjected to seismic loads. In the capacity spectrum method the capacity curve is obtained by using NLSP and is overlapped with the inelastic demand curve to obtain the performance point. Displacement coefficient method is a simple method for estimating the target displacement. Target displacement refers to the displacement of a characteristic node, specifically on the top of a structure. Fig. 2 and 3 presents the PBSE procedures.

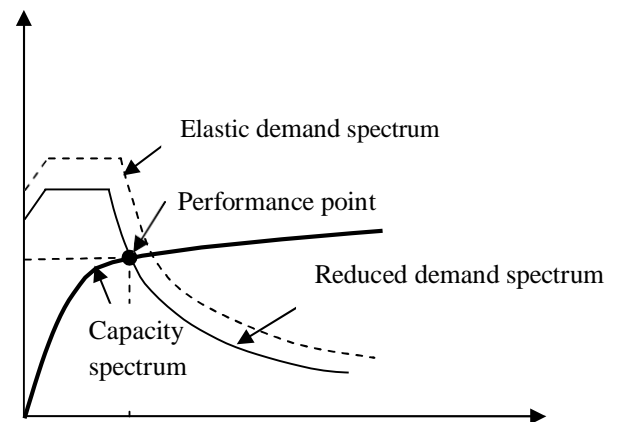


Fig. 2: Determination of performance point as per CSM procedures

The accuracy of NLSP depends on the inelastic modelling of reinforced concrete members. The inelastic characteristics of the reinforced concrete members are introduced by assigning the plastic hinges. PBSE put forth two actions of plastic hinges viz. deformation-controlled (ductile action) or force-controlled (brittle action). In the present study the effects of axial force on beams were disregarded, considering the presence of rigid diaphragms. However, these effects were considered for the columns. Fig. 4 and Table 3-4 gives details of plastic rotation limits for reinforced concrete beams and columns described in PBSE documents.

In this study, we performed displacement-controlled NLSP

on the example MRFs by using SAP 2000 V 20.0 (Wilson and Habibullah, 2000). The target displacement used for each MRF was 4% of the height of the frame (ATC 40, 1996). The analysis was conducted in two stages for the following: (i) gravity loads and (ii) predominant lateral loads.

Table 1: Structural irregularities defined in IS 1893: 2002

Sr, No.	Types of Irregularity	Classification	Limits
1	Torsion irregularity	Plan irregularity	$e_{max}=1.2\Delta_{avg}$
2	Diaphragms irregularity	Plan irregularity	$D_i = 0.50$ Gross diaphragms area
3	Stiffness irregularity A) Soft storey B) Extreme soft storey	Vertical Irregularity	$S_i < 0.70 S_a$ or $S_i < 0.80 S_{3avg}$ $S_i < 0.60 S_a$ or $S_i < 0.70 S_{3avg}$
4	Mass irregularity	Vertical Irregularity	$M_i < 2.0 M_a$
5	Vertically geometric irregularity	Vertical Irregularity	$V_g < 1.5 V_{ga}$
6	Discontinuity in capacity weak storey	Vertical Irregularity	Strength < 0.80 times the Strength of the above floor

Where ‘a’ states the adjacent storey number, Δ_{avg} is average displacement of adjacent stories and 3_{avg} implies average of three storeys

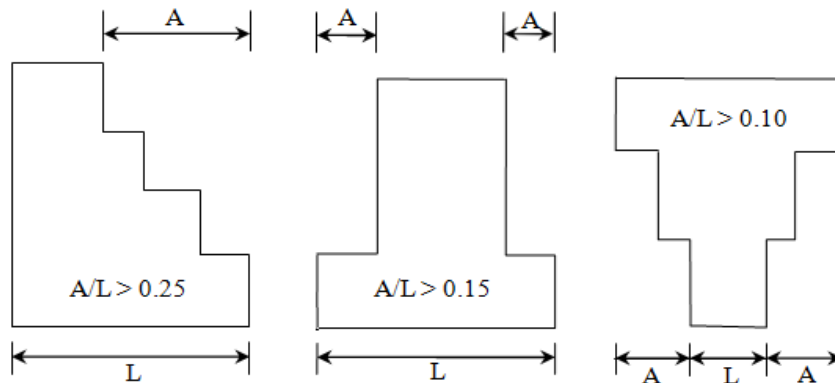


Fig.1: Vertical geometric irregularity as per IS 1893:2002

In Stage I, gravity loads were applied as the distributed element loads on the basis of the yield line theory and concentrated loads from secondary beams. Gravity analysis was performed for full gravity load in a single step (i.e., force-control). The state of the structure in this analysis was saved and was subsequently recalled in Stage II. In Stage II, lateral loads were applied monotonically in a step by-step nonlinear static analysis. Because the lateral force profile in pushover analysis influences the structural response. IS1893:2002 trivial lateral load patterns were applied.

EXAMPLE MRFs

The example MRFs considered for this study represents regular and irregular frames along vertical profile. The vertical irregularities is introduced in the MRFs in accordance to the guidelines of IS 1893:2002. Table 5

provides the details of example MRFs. These MRFs are considered to be bare frames located in the zone V (zone factor, 0.36) which is the severest zone as per IS 1893 and soil type is medium. The structure importance factor used is 1.0. The modification factor of 5 was used to account for the ductility in MRFs.

Fig. 5: shows the typical layout of the example MRFs. Three different types of vertically irregularities have been considered in the present work which, are commonly found in urban constructions. Vertical irregularity introduced represents set-back of 20 and 40 percent of the plan width of the structure. Similar regular building having no unusual irregularity in spatial form have been studied for benchmark the results of the parametric studies.

For the analysis, the dead loads, live (imposed) loads, and

seismic loads on example MRFs were considered as per IS 875 (Part 1 and 2) (1987) and IS 1893 (2002), respectively. These MRFs carries a mean dead load of 40 kN/m, inclusive of the finishes loads and a mean live load of 9 kN/m, for all floors. The design of reinforced concrete

sections is done following the guidelines of IS 456 and their detailing is done as per IS 13920 specifications. Table 6 provides the material properties and design constants used in the design. Table 7-8 shows the design details of the reinforced concrete sections.

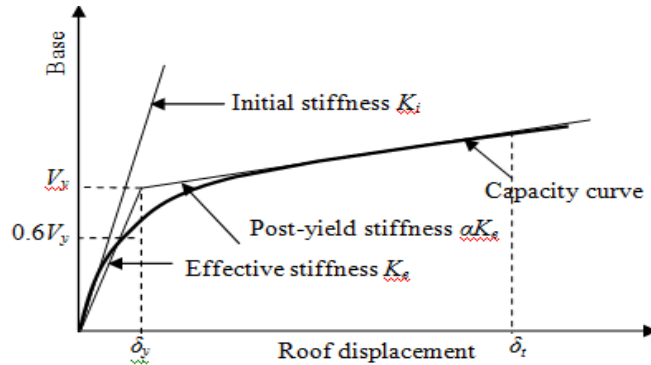


Fig. 3: Calculation of target displacement as per DCM

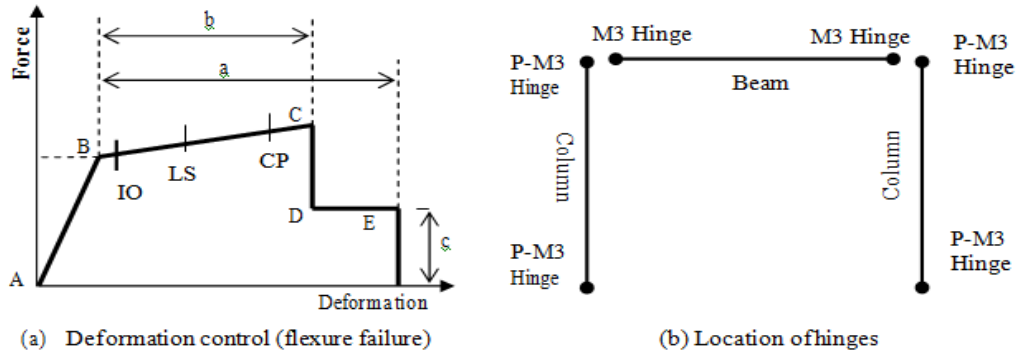


Fig. 4: Idealized inelastic force–deformation relationship

Table 3: Plastic rotation limits for RC beams controlled by flexure (FEMA 356)

CONDITIONS			Modelling Parameters			Acceptance Criteria				
			Plastic rotation angle (radians)		Residual strength ratio	Plastic rotation angle (radians)				
$\frac{P}{A_g f'_c}$	Trans. Reinf.	$\frac{V}{b_w d \sqrt{f'_c}}$	a	b		c	IO	Performance level		
					Component type					
			LS	CP	LS	CP				
≤ 0.5	C	≤ 3	0.02	0.03	0.2	0.005	0.010	0.02	0.02	0.03

C indicates the transverse reinforcement meets the criteria for ductile detailing

Table 4: Plastic rotation limits for RC columns controlled by flexure (FEMA 356)

CONDITIONS			Modelling Parameters			Acceptance Criteria				
			Plastic rotation angle (radians)		Residual strength ratio	Plastic rotation angle (radians)				
$\frac{P}{A_g f'_c}$	Trans. Reinf.	$\frac{V}{b_w d \sqrt{f'_c}}$	a	b		c	IO	Performance level		
					Component type					
			LS	CP	LS	CP				
≥ 0.1	C	≤ 3	0.02	0.03	0.2	0.005	0.015	0.02	0.02	0.03

C indicates the transverse reinforcement meets the criteria for ductile detailing

Table 5: Details of example MRFs used in the study

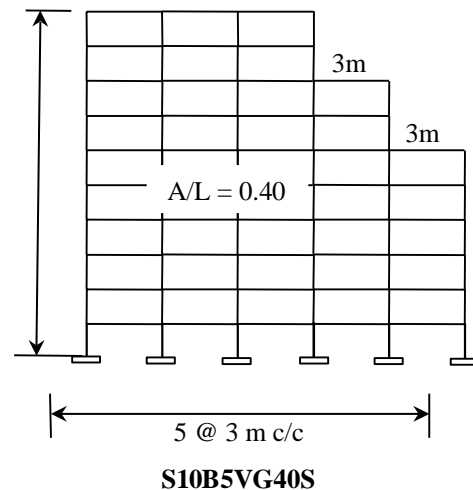
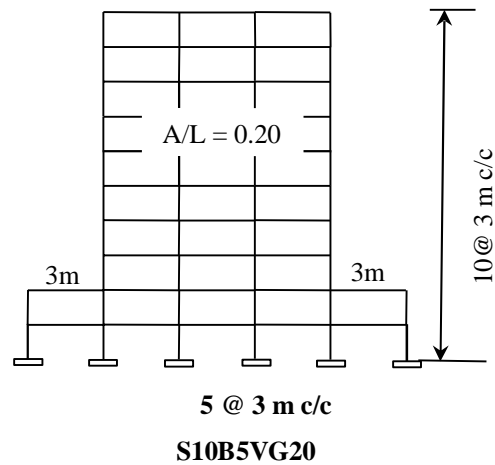
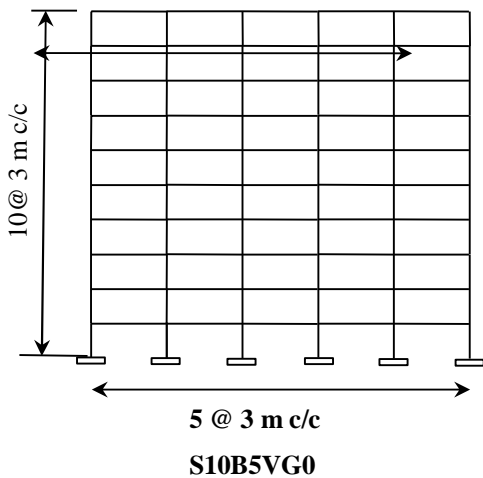
Frames	Height (m)	T _d (s)	W _i (kN)	A _h = V _d /W	V _d (kN)
S10B5VG0	30	0.961	7064.08	0.05	359.78
S10B5VG20	30	0.961	4864.12	0.05	247.73
S10B5VG40S	30	0.961	6334.06	0.05	322.60
S10B5VG40T	30	0.961	6469.37	0.05	329.49

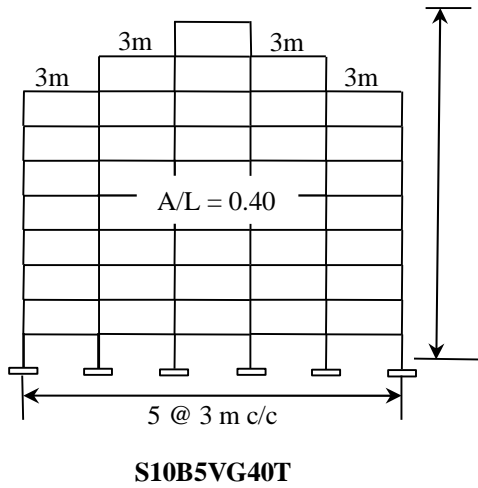
S represents No. of storey, B says the number of bays and VG shows vertical irregularities of different type and percentages

Table 6: Material properties considered in the design of example MRF [IS456, IS1786]

Material property	Concrete	Steel
	M 25 Grade	Fe 415 grade
Weight per unit volume (kN/m ³)	25	76.97
Mass per unit volume (kN/m ³)	2.548	7.849
Modulus of elasticity (kN/m ²)	25E+06	2E+08
Characteristic strength (kN/m ²)	25000 (for 28 days)	415000 (yield)
Minimum tensile strength (kN/m ²)	-	485800
Expected yield strength (kN/m ²)	-	456500
Expected tensile strength(kN/m ²)	-	533500

The structural design of the example MRFs is not a unique solution available for the calculated demand. Based on the same demand, different designers may select different solutions. The RC member sizes were selected by following a common practice adopted by engineers. All the columns and beams in a selected story are identical in cross section. The column remained uniform in cross section up to two or three stories, depending on the height of the building. Table 9 describes the modal analysis results of example MRFs.





S10B5VG40T

Fig. 5: Selected vertical irregular buildings

PARAMETRIC STUDIES

The performance-based seismic design has two primary concerns: (a) appropriate quantification of the uncertainties associated with the performance evaluation process, and (b) satisfactory characterization of the associated structural damage for direct incorporation into the design or performance evaluation methodology [Zameeruddin and Sangle, 2021]. The performance of example MRFs is evaluated on the basis of the parametric studies done on the fundamental period of vibration, base shear, roof displacement, story displacement, and inter-story drift ratio.

Table 7: Summary of designed column section for example MRF

Example MRFs	Storey No	External /Internal column		Beams	
		size (mm)	Rebar's (mm ²)	size (mm)	Rebar's (mm ²)
For all MRFs	1-3	300 x 600	4910	300 x 450	Default values
	4-6	300 x 530	3920	300 x 450	provided by
	7-10	300 x 450	2946	300 x 380	SAP 2000 V 20.0

Table 8: Modal Analysis results of studied example MRFs

Storey Level	S10B5VG0				S10B5VG20			
	Modal time Period (T _m)	Modal Frequency cycles/sec	Stiffness (kN/mm)	Lateral Loads (kN)	Modal time Period (T _m)	Modal Frequency cycles/sec	Stiffness (kN/mm)	Lateral Loads (kN)
1	1.428	0.699	361.35	1.10	1.345	0.743	361.35	1.24
2	0.504	1.980	361.35	4.43	0.483	2.068	361.35	4.89
3	0.287	3.474	361.35	9.90	0.282	3.534	240.81	6.76
4	0.192	5.197	249.48	17.49	0.194	5.144	166.23	11.94
5	0.140	7.101	249.48	27.34	0.141	7.087	166.23	18.66
6	0.126	7.913	249.08	39.08	0.121	8.244	165.99	26.66
7	0.115	8.649	152.82	52.81	0.109	9.157	101.82	36.00
8	0.111	9.000	152.82	68.13	0.101	9.893	101.82	46.45
9	0.102	9.764	152.82	86.23	0.086	11.60	101.82	58.79
10	0.090	10.975	152.82	53.23	0.083	12.04	101.82	36.29

Table 9: Modal Analysis results of studied example MRFs

Storey Level	S10B5VG40S				S10B5VG40T			
	Modal time Period (T _m)	Modal Frequency cycles/sec	Stiffness (kN/mm)	Lateral Loads (kN)	Modal time Period (T _m)	Modal Frequency cycles/sec	Stiffness (kN/mm)	Lateral Loads (kN)
1	1.284	0.778	361.35	1.275	1.288	0.776	361.35	1.296
2	0.497	2.00	361.35	5.10	0.451	2.215	361.35	5.182
3	0.287	3.481	361.35	11.40	0.271	3.681	361.35	11.58
4	0.196	5.084	249.48	20.14	0.189	5.282	249.48	20.47

5	0.142	7.033	249.48	31.48	0.140	7.106	249.48	31.98
6	0.122	8.138	249.08	44.69	0.121	8.264	249.08	45.72
7	0.110	9.030	127.32	48.81	0.115	8.692	152.82	61.78
8	0.105	9.460	127.32	62.43	0.104	9.556	152.82	78.61
9	0.092	10.758	101.82	60.12	0.097	10.24	101.82	59.69
10	0.089	11.145	101.82	37.11	0.095	10.50	50.81	13.14

The natural period of vibration, of example MRFs evaluated from the empirical equation given in IS 1893 for the buildings without infills, is presented in Table 5. Also, modal analysis of the example MRFs has been performed to determine a fundamental period of vibration by using Eigen values; the results are reported in Table 8-9. The fundamental period is the first-mode longest modal time period of vibration. The fundamental period obtained from the Eigen value analysis is found to be higher than the values derived using the code empirical relation. The difference in the time period of vibration (reported in Table 10) can be attributed towards the changes in the cross-sectional areas of RC members and the span of member of a building which is not taken in to account by the IS code empirical relationship. A modal participating mass ratio shown in Table 11 describes the correlation between higher mode participation and irregularity. The NLSP was performed on the example MRFs for lateral load distribution obtained with reference to IS 1893:2002 guidelines using SAP 2000 V 20. The results of NLSP are shown in the form of the pushover curves, which are typically the base force versus roof displacement plot. Fig.

6 shows pushover curves of the example MRFs. The intersection of capacity curve with the inelastic demand spectra gives the performance point. Table 12 gives the values of the base force and displacement obtained at the performance point for various PBSE methods applied to example MRFs

The values of the roof displacement obtained from various PBSE methods showed that the displacement of MRF with set-back vertical irregularity is largest one compare to other type of example irregular MRFs.

Fig 7 represents the collapse mechanism of the example MRFs showing the yield of plastic hinges from one performance level to other performance level. In PBSD the performance levels are defined in terms of damages sustain by the structural and non-structural components of a structure during a seismic event, namely Operational (OP), Immediate Occupancy (IO), Life Safety range (LS), Collapse Prevention (CP) and Collapse (C).

Table 10: Modal Analysis results of studied example MRFs

Example MRF	T_m	T_d	Difference (%) = [(T_m-T_d)/T_d]*100
S10B5VG0	1.428	0.96	+ 48.80
S10B5VG20	1.345	0.96	+ 40.10
S10B5VG40S	1.284	0.96	+ 33.80
S10B5VG40T	1.288	0.96	+ 34.20

Table 11: Modal Participation factors of studied example MRFs

Example MRF	Mode1	Mode 2	Mode 3
S10B5VG0	0.77	0.11	0.04
S10B5VG20	0.66	0.14	0.08
S10B5VG40S	0.76	0.10	0.05
S10B5VG40T	0.77	0.10	0.04

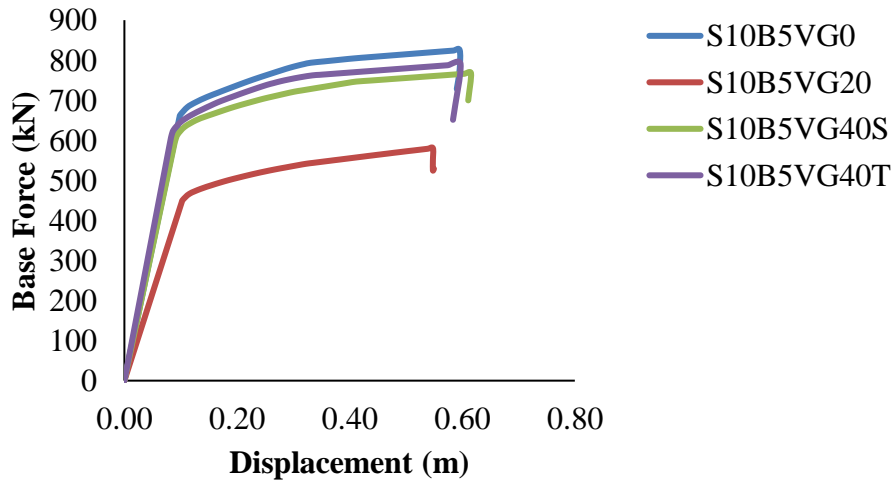


Fig 6: Pushover curves of example MRFs

Table 12: Base force and displacement at performance point for various PBSE methods

PBSE Methods	ATC 40 (CSM)		FEMA 356 (DCM)		FEMA 440 (ACSM)		FEMA 440 (MDCM/)	
	V _p , (kN)	d _p , (m)	V _p , (kN)	d _p , (m)	V _p , (kN)	d _p , (m)	V _p , (kN)	d _p , (m)
S10B5VG0	719.35	0.167	789.69	0.317	721.68	0.171	789.69	0.317
S10B5VG20	491.22	0.162	538.57	0.311	493.76	0.168	538.57	0.311
S10B5VG40S	668.55	0.163	724.78	0.316	670.35	0.167	724.78	0.316
S10B5VG40T	688.78	0.156	754.29	0.301	691.07	0.160	754.29	0.301

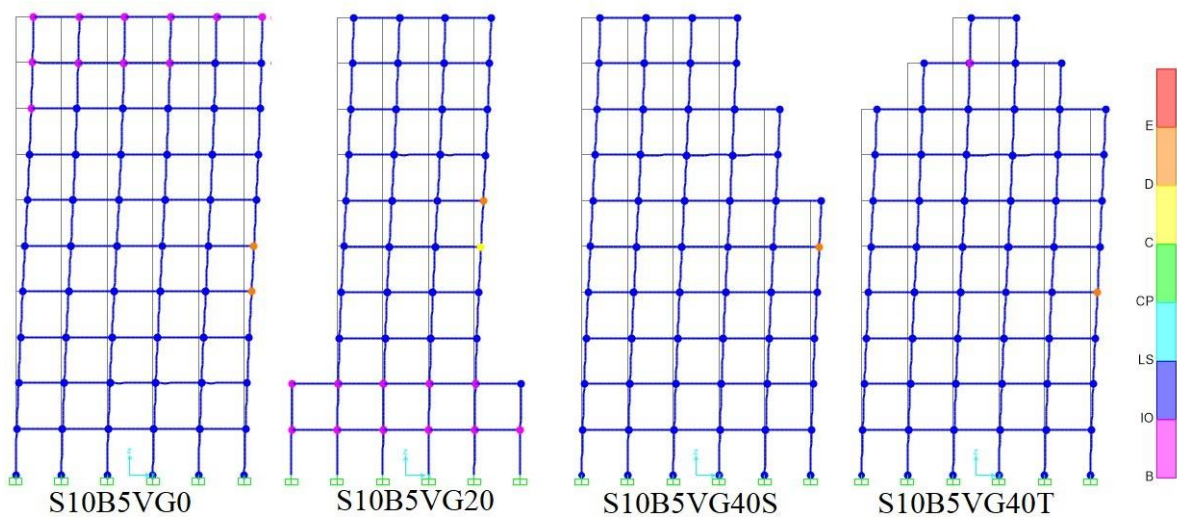


Fig. 7: Plastic hinge mechanism of example MRFs

The story drift is a useful and simple measure of the overall structural deformation that is routinely examined. Fig. 9 illustrates that storey displacement and Fig. 10 presents the inter-story drift ratio of the example MRFs. It was observed that the set-back vertical irregularities are on

higher values displacements compare to the other type of irregularities. The storey displacement and inter-story may help a designer to choose a type of vertical irregularities to be introduced in a unavoidable situations.

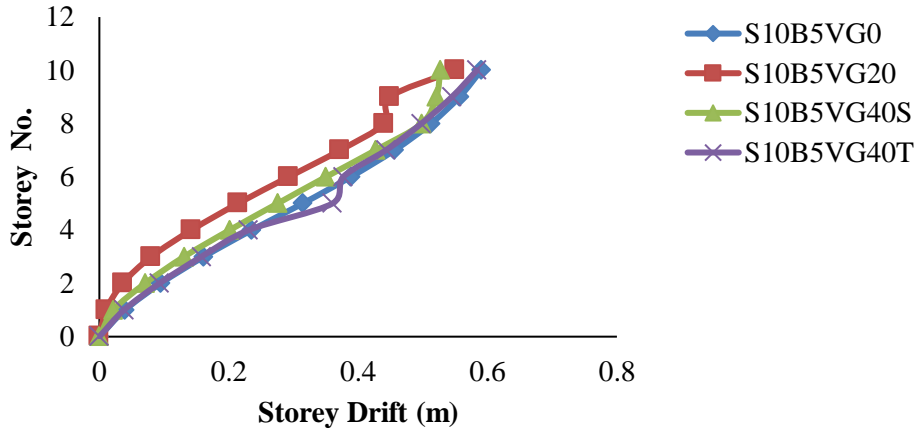


Fig. 9: Storey displacements of example MRFs

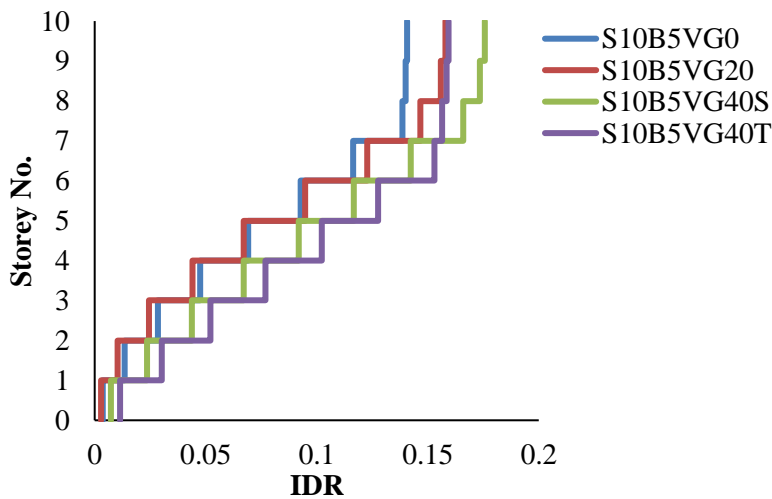


Fig. 10: Inter-story drift ratio of example MRFs

To evaluate the damages for example MRFs two performance indicator levels is proposed (a) PL1 – which includes OP and IO levels as damages to structural components are repairable and no threat to life (b) PL2- which includes LS, CP and C levels as damages to structural components are irreparable, downtime for usage and risk to life is involved. The ductility ratio (μ) and overstrength (Ω) derived from pushover results at PL1 and PL2 are given in Table 13-14.

Table 13: Pushover parameters for PL1 (considering P- Δ) effects

Example MRFs	V_d (kN)	V_u (kN)	VPL1 (kN)	d_y (m)	d_u (m)	dPL1 (m)	$\mu = d_u/d_y$	$\Omega = V_u/V_y$	$\mu' = du/dPL1$	$\Omega' = VU/VPL1$
S10B5VG0	359.78	825.8	737.77	0.178	0.595	0.201	3.34	2.30	1.13	2.05
S10B5VG20	247.73	580.38	443.66	0.096	0.55	0.101	5.73	2.34	1.05	1.79
S10B5VG40S	322.6	767.28	588.6	0.084	0.616	0.089	7.33	2.38	1.06	1.82
S10B5VG40T	329.49	789.83	708.77	0.18	0.597	0.192	3.32	2.40	1.07	2.15

Table 14: Pushover parameters for PL2 (considering P-Δ) effects

Example MRFs	V _d (kN)	V _u (kN)	V _{P2} (kN)	d _y (m)	d _u (m)	d _{P2} (m)	μ = d _u /d _y	Ω = V _u /V _y	μ' = d _u /d _{P1}	Ω' = V _U /V _{P1}
S10B5VG0	359.78	825.8	825.8	0.178	0.595	0.595	3.34	2.30	3.34	2.30
S10B5VG20	247.73	580.3	506.93	0.096	0.550	0.230	5.73	2.34	2.40	2.05
S10B5VG40S	322.6	767.28	690.9	0.084	0.616	0.213	7.33	2.38	2.54	2.14
S10B5VG40T	329.49	789.83	789.8	0.180	0.597	0.597	3.32	2.40	3.32	2.40

In its present form PBSE procedures are capable to provide the plastic hinge collapse mechanism, but are not able to provide any associated damage value. Many researchers have provided damage index using response parameters yield from NLSP and Nonlinear dynamic procedures, but still they are not been common in practice

due to complex assessment procedures [Zameeruddin and Sangale, 2017b, 2017c, 2020; Mihaită, 2015; Powell and Allahbadi, 1988]. In this study, we have attempted to evaluate the damage to the example MRFs using loss of stiffness during pushover.

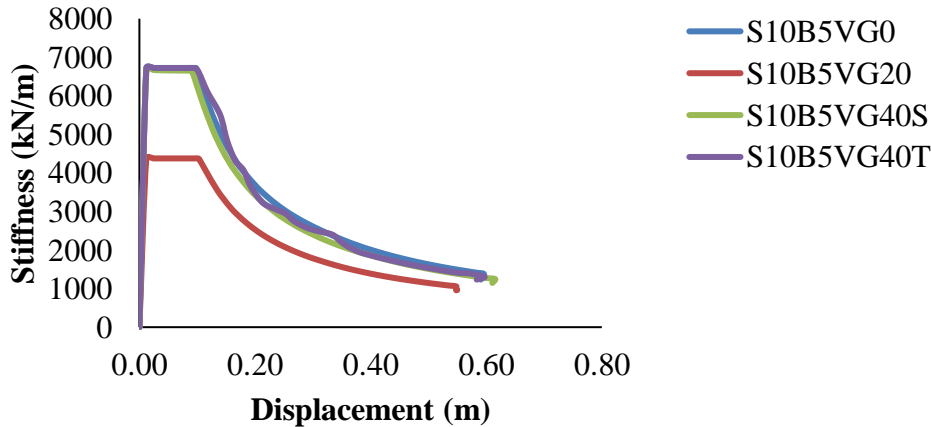


Fig. 8: Loss of stiffness during pushover

Fig. 8 shows the loss of stiffness during a pushover analysis. Table 15-16 gives the values of parameters used in the evaluation of damage value. The damage indicator are calibrated based on stiffness and drift values obtained at yield, PL1, PL2 and collapse state of example MRFs when subjected to pushover. The damage indicator presents the loss of stiffness and ductility at identified performance levels. The empirical relationships used are;

$$DI_{\mu PL1} = 1 - (K_{PL1} / K_{op})$$

$$DI_{\mu PL2} = 1 - (K_{PL2} / K_{op})$$

Where K_{op} is stiffness of structure in operational level; K_{PL1} and K_{PL2} are the stiffness of structure at PL1 and PL2

$$DI_{\mu PL1} = 1 - [(d_{PL1} - d_y) / (d_u - d_y)]$$

$$DI_{\mu PL2} = 1 - [(d_{PL2} - d_y) / (d_u - d_y)]$$

Where d_y, d_{PL1}, d_{PL2} and d_u are the values of displacements at yield, PL1, PL2 and ultimate state.

Table 15: Calculation of stiffness and drift based damage values at PL1

Example MRFs	K _{op}	K _{PL1}	K _{PL2}	DI _{kPL1}	DI _{kPL2}
S10B5VG0	4072.56	3670.50	1387.90	0.10	0.659
S10B5VG20	4376.41	4392.67	2204.04	0.00	0.496
S10B5VG40S	6653.94	6616.40	3243.66	0.01	0.513
S10B5VG40T	3903.67	3691.51	1322.95	0.05	0.661

Table 16: Calculation of stiffness and drift based damage values at PL2

Example MRFs	d_y (m)	d_n (m)	dPL1 (m)	dPL2 (m)	DI $_{\mu}$ PL1	DI $_{\mu}$ PL2
S10B5VG0	0.178	0.595	0.201	0.595	0.945	0.00
S10B5VG20	0.096	0.550	0.101	0.230	0.989	0.70
S10B5VG40S	0.089	0.616	0.089	0.213	1.000	0.76
S10B5VG40T	0.18	0.597	0.192	0.597	0.971	0.00

Conclusions

With the increasing demand of functional and aesthetic architecture a complex shaped structures are becoming very common. The complex shaped geometry has introduced horizontal and vertical irregularities in a structure in terms of mass, stiffness and strength. When these structures were subjected to seismic loads they were severely damaged or collapse demanding seismic evaluation and damage assessment. PBSB has emerged as best alternative towards present seismic codes which states multiple performance levels under seismic hazards. In present study, the performance evaluation and damage assessment of vertically irregular buildings were studied under the guidelines of PBSB document. The conclusion drawn from these studies are;

1. IS 1893 provides the empirical relation to estimate the fundamental period of vibration to estimate inertia loads acting on a structure. The fundamental period obtained from the Eigen value analysis is found to be higher than the values derived using the code empirical relation. This difference in the time period of vibration can be attributed towards the changes in the cross-sectional areas of RC members and the span of member of a building which is not taken in to account by the IS code empirical relationship.
2. A modal participating mass ratio describes the correlation between higher mode participation and irregularity. Building with set-back irregularity shows higher first mode participation factor compare to other type of vertical irregularity studied.
3. Various performance evaluation methods described in PBSB document were use to evaluate the performance of structure. The values of the roof displacement obtained from these PBSE methods at performance point showed that the displacement of MRF with set-back vertical irregularity is largest one compare to other type of example irregular MRFs.
4. The primary concern of PBSB is to evaluate

the performance of structure and assess the damages sustain by the structure. In its present state the PBSE methods are capable to evaluate the yield mechanism but do not convey any damage values.

5. Within the dimension of performance levels defined in PBSE, some performance indicator levels are grouped to show global damages to the structure as PL1 and PL2. PL1 uses OP and IO performance levels where repairs and less threat to life are assured, while PL2 uses LS, CP and C performance levels in which irreparable damages, downtime for usage and life loss is considered.
6. When these performance indicator levels PL1 and PL2 were evaluated using damage indicator based on loss of stiffness and ductility. There is a possibility of scaling the damage in a scale of 0 to 1.

The study performed is within small scale of example studies which can be executed on larger domain addressing other types of structural irregularities within a domain of PBSB. A attempt has been made to integrate PBSE method with damage indicator which is a gray area of research in structural engineering using NLSP.

Declaration of Competing Interest

The authors declare that they have no known competing financial interests or personal relationships that could have appeared to influence the work reported in this paper.

Acknowledgement

The authors of this paper acknowledge the research contributions of all the citations under reference.

References

- [1] ASCE/SEI 41. American Society of Civil Engineers. Seismic rehabilitation of existing building; 2007[Reston, Virginia].
- [2] ATC-40. Seismic evaluation and retrofit of existing concrete buildings. Redwood City (CA): Applied Technical Council; 1996.
- [3] Bhosale A. S., Davis R and Sarkar P. (2017). ASCE-ASME. J. Risk Uncertainty Eng. Syst. Part A: Civ. Eng., 03 (3): 04017001-10. <https://doi.org/10.1061/AJRUA6.0000900>
- [4] BIS IS 1893. Indian standard criteria for earthquake resistant design of structures (part 1): general provisions and buildings (fifth revision). New Delhi: Bureau of Indian Standards; 2002.
- [5] Boroujeni ARK. Evaluation of various methods of FEMA 356 compare to FEMA 440. J Civ Eng Constr Technol 2013;4(2):51-5. <http://dx.doi.org/10.5897/JCECT12.082>
- [6] FEMA 273. NEHRP guidelines for the seismic rehabilitation of buildings. Washington (DC): Federal Emergency Management Agency; 1996.
- [7] FEMA 356. Pre-standard and commentary for the seismic rehabilitation of buildings. Washington (DC): Federal Emergency Management Agency; 2000.
- [8] FEMA 445, 2006. Next-generation performance-based seismic design guideline program for new and existing buildings. Federal Emergency Management Agency, Washington (DC).
- [9] FEMA 445. Next generation performance based seismic design guidelines: program plan for new and existing buildings.

- Washington (DC): Federal Emergency Management Agency; 2006.
- [10] Ghobarah A. Performance-based design in earthquake engineering: state of development. *Eng Struct* 2001; 23:878–84. [https://doi.org/10.1016/S0141-0296\(01\)00036-0](https://doi.org/10.1016/S0141-0296(01)00036-0)
- [11] IS 13920, 1993. Ductile detailing of reinforced concrete structures subjected to seismic force-code of practice. Bureau of Indian standards, New Delhi.
- [12] IS 1786, 2008. Indian standard for high strength deformed steel bars and wires for concrete reinforcement. Bureau of Indian standards, New Delhi.
- [13] IS 456, 2000. Indian standard plain and reinforced concrete – code of practice (fourth revision). Bureau of Indian standards, New Delhi.
- [14] IS 875, 1987. Code of practice for design loads (other than earthquake) for buildings and structures: part 1 dead loads. Bureau of Indian standards, New Delhi.
- [15] IS 875, 1987. Code of practice for design loads (other than earthquake) for buildings and structures: part 2 imposed loads. Bureau of Indian standards, New Delhi.
- [16] Mondal, A., Ghosh, S., Reddy, G.R., 2013. Performance-based evaluation of the response reduction factor for ductile RC frames. *Eng. Struct.* 56, 1808–1819. <https://doi.org/10.1016/j.engstruct.2013.07.038>
- [17] Siva N. E., Abraham N. M., and S. D. Anitha., 2019. Analysis of irregular structures under earthquake loads. *Procedia Structural Integrity*, 14, 806-819. <https://doi.org/10.1016/j.prostr.2019.07.059>
- [18] Soni D. P. and Mistry B. B. (2006). Qualitative review on seismic response of vertically irregular building frames. *ISET journal of earthquake technology*, Technical Note. 43 (4): 121-132.
- [19] Valmundsson, E. V., & Nau, J. M. (1997). Seismic response of building frames with vertical structural irregularities. *Journal of Structural Engineering*, 123(1), 30–41. [https://doi.org/10.1061/\(ASCE\)0733-9445\(1997\)123:1\(30\)](https://doi.org/10.1061/(ASCE)0733-9445(1997)123:1(30))
- [20] Wilson, E.L., Habibullah, A., 2000. SAP 2000/NL-push version 17 software, computer and structures, Inc, Berkeley, CA, USA
- [21] Zameeruddin, M., Sangle, K.K., 2016. Review on recent developments in performance- based seismic design of reinforced concrete structures. *Structures* 6, 119–133. <https://doi.org/10.1016/j.istruct.2016.03.001>
- [22] Zameeruddin, M., Sangle, K.K., 2017a. Seismic performance evaluation of reinforced concrete frames subjected to seismic loads. *J. Inst. Eng. India Ser. A* 98, 177–183. <https://doi.org/10.1007/s40030-017-0196-0>.
- [23] Zameeruddin, M., Sangle, K.K., 2017b. Seismic damage assessment of reinforced concrete structure using nonlinear static analyses. *KSCE J. Civil Eng.* 21 (4), 1319–1330. <https://doi.org/10.1007/s12205-016-0541-2>.
- [24] Zameeruddin, M., Sangle, K.K., 2017c. Energy-based damage assessment of RCMRFs using pushover. *Asian J. Civil Eng. (BHRC)* 18 (7), 1077–1093.
- [25] Zameeruddin, M, Sangle, K K, 2021. Performance-based seismic assessment of reinforced concrete frames. *J. King Saud Univ. Eng. Sci.*, 33(3):153-165. <https://doi.org/10.1016/j.jksues.2020.04.005>
- [26] Zameeruddin, M, Sangle, K K, (In press). Damage assessment of reinforced concrete moment resisting frames using performance-based seismic evaluation procedures. *J. King Saud Univ. Eng. Sci.* <https://doi.org/10.1016/j.jksues.2020.04.010>
- [27] Powell, G H, Allahabadi, R, 1988. Seismic damage prediction by deterministic methods: concept and procedure. *Earthq. Eng. Struct. Dyn.* 16 (5), 719–734.
- [29] Mihai, Mihaită, 2015. A theoretical review of the damage indices used to model the dynamic behavior of reinforced concrete structures. *Bull. Polytech. Inst. Lasi Constr. Architect. Sect.* 63 (2), 109–119.